Brightness and color variation for evening and morning twilights at Bahria of Egypt IV

CrossMark

A.H. Hassan, Yasser A. Abdel-Hadi *, I.A. Issa, N.Y. Hassanin

National Research Institute of Astronomy and Geophysics, Helwan, Cairo, Egypt

Abstract Photoelectric observations of twilight (evening and morning) Bahria ($\varphi = 28°\ 42.94'$ N, $\lambda = 28°\ 59.99'$ E) in Egypt were done in the period between 1983 and 1985. A semiautomatic photoelectric scanner equipped with a refractor of diameter $D = 10$ cm and focal length $f = 24$ cm was used. The phenomena were followed in altitude and azimuth each 10°. For evening twilight, we find a minimum value in the color index (CI) curves at $D_o = 12.5°$. The color index (CI) is found to be in the range between -1.5 and 3. A decrease on both sides of the CI toward large and small depressions is seen indicating a red background. This red color decreases on both sides of the maximum although being positive. No change of the maximum values is noticed with the azimuth. The (B–R) curves show positive maximum values at $11° \leqslant D_o \leqslant 13°$ with a decrease on both sides. Color indices are studied for the three bands (B–V), (B–R) and (V–R) for morning and evening twilights. For morning twilight, the (B–V) color index curves show minimum (CI) values with positive (B–V) at D_o around 8°. This can denote a dominating yellow color of the sky till $D_o \approx 8$–10°, where the sky is as bright in the yellow as in the blue. Stability is reached at $D_o = 12$–14°. We believe that, the dawn shows itself at $D_o \leqslant 15°$, while the nightfall shows itself at $D_o \leqslant 18°$.
© 2014 Production and hosting by Elsevier B.V. on behalf of National Research Institute of Astronomy and Geophysics.

1. Introduction

Human activities are controlled mostly by the position of the sun above the horizon and to some extent below the horizon.

* Corresponding author. Tel.: +20 1000556473; fax: +20 225548020.
  E-mail address: yasser_hadi@yahoo.com (Y.A. Abdel-Hadi).
Peer review under responsibility of National Research Institute of Astronomy and Geophysics.

The brightness in direct sunlight in day is $\sim 10^6$ times the brightness at night. According to Rayleigh law, where the intensity of the scattered light is proportional to λ^{-4}, the ratio of the intensity of the scattered blue light to that of the red light is 16. This answers the question why the sky appears blue, Rosenberg (1966), McGillivray (1987), Roach and Gordon (1973), Aden and Meinel (1991).

The human eye is sensitive over the wavelength range from 350 nm to 750 nm. The lowest energy that can be detected by the normal young eye ranges between 3.3×10^{-17} and 6.6×10^{-17} Joule. According to $E = nh\upsilon$ and at $\lambda = 507$ nm, it was calculated that the eye needs on the average between 84 and 168 photons striking the cornea to feel light. Nearly and according to physiological and statistical studies about
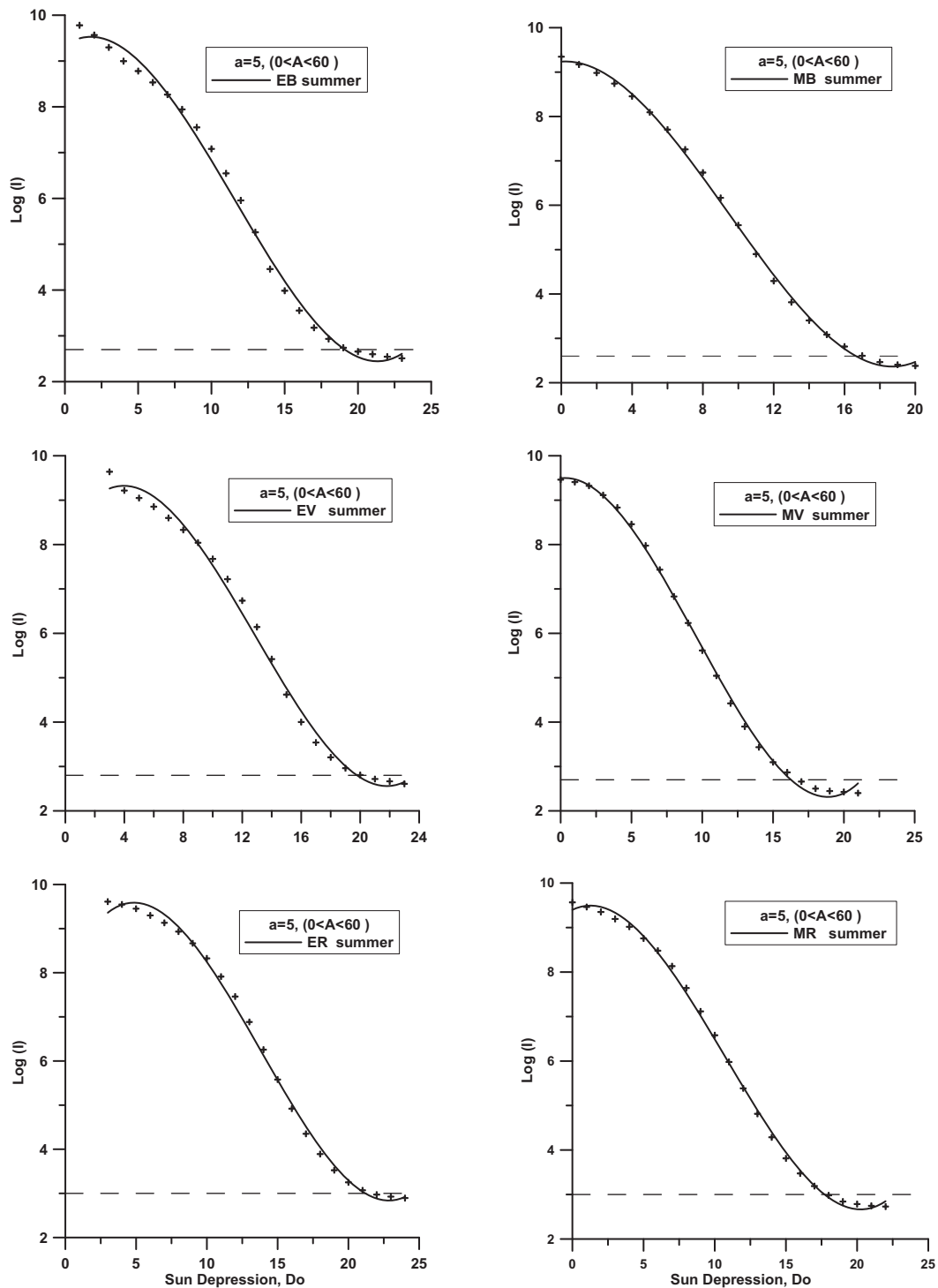
Fig. 1 The relation between *Log (I)* expressed in S_{10} units (*B, V & R*) and the sun's depression (D_o) at Bahria, for evening (*E*) and morning (*M*) twilights azimuth averaged over ($0° \leqslant A \leqslant 60°$) and at altitude, $a = 5°$ for summer season.

5–10 photons are enough to excite the rods of the dark adapted eye to be stimulated, Richard (1946), Belikov (1996), Valberg (2005).

Twilight observations and studies have been carried out by many scientists, Rosenberg (1966), Gadsden (1966), Asaad et al. (1974), Asaad et al. (1977), Nawar (1983, 1995), Issa and Hassan (2008, II & III). Extinction observations and studies have been published by Mikhail (1979, I and II), Issa and Hassan (2008, I), Issa et al. (2011), Hassan et al. (2013). The method, the technique of observations, the procedure of data analysis, reduction, acquisition together with the extinction Hardie (1962) and brightness curves have
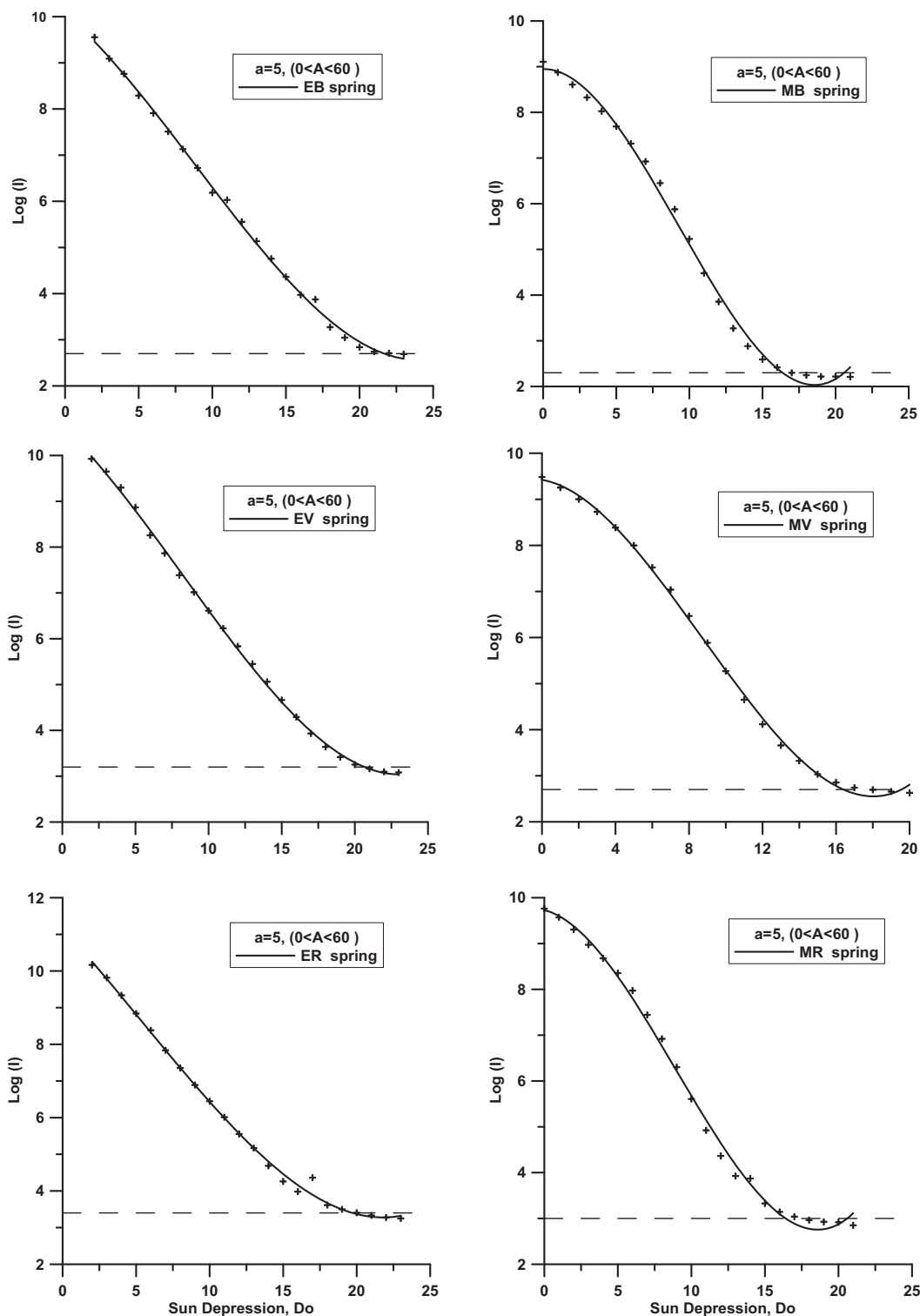
Fig. 2 The relation between $Log\ (I)$ expressed in S_{10} units (B, V & R) and the sun's depression (D_o) at Bahria, for evening (E) and morning (M) twilights azimuth averaged over ($0° \leqslant A \leqslant 60°$) and at altitude, $a = 5°$ for spring season.

been published early by Issa and Hassan (2008, I, II and III).

In the present work, we give some trials to express the twilight brightness data in a mathematical form Hardie (1962).

We want to get a formula that can expect the phenomena to the nearest fraction of degree. This study presents observations taken in summer and spring in 1984. We reanalyze the brightness data, the color indices both as a function of the depression

Table 1 The constants of a 3rd degree polynomial for evening (E) and morning (M) for the colors (B, V & R) in summer and spring.

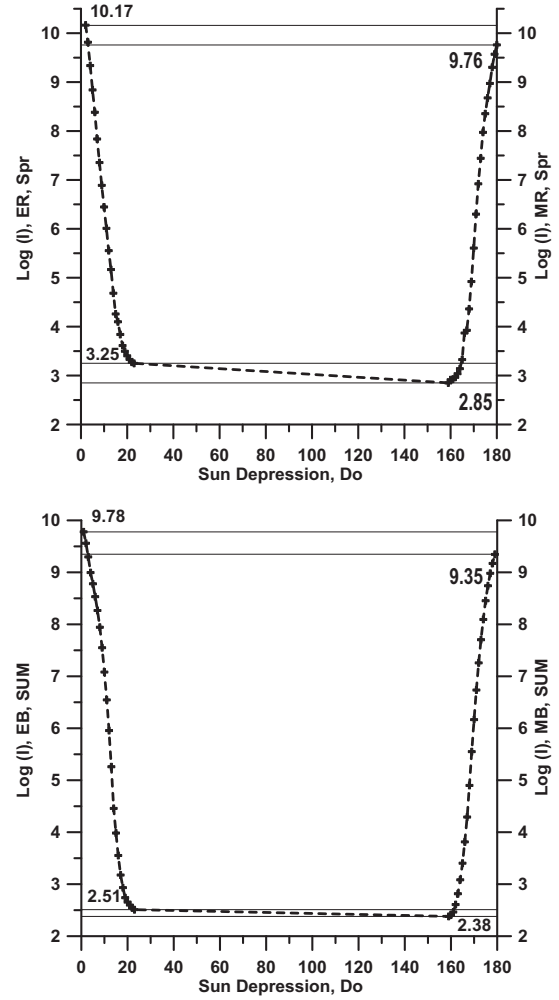| Color	Summer				Spring			
	c_o	$c_1 \, deg^{-1}$	$c_2 \, deg^{-2}$	$c_3 \, deg^{-3}$	c_o	$c_1 \, deg^{-1}$	$c_2 \, deg^{-2}$	$c_3 \, deg^{-3}$
EB	9.342	.215	−0.066	0.002	10.174	−0.321	−0.011	0.0004
EV	8.172	0.619	−0.092	0.002	10.641	−0.303	−0.017	0.0007
ER	7.86	0.767	−0.096	0.002	11.111	−0.413	−0.012	0.0007
MB	9.236	0.032	−0.062	0.002	8.946	0.009	−0.061	0.0022
MV	9.493	0.043	−0.065	0.002	9.423	−0.068	−0.056	0.0021
MR	9.391	0.16	−0.065	0.002	9.728	−0.077	−0.052	0.0019
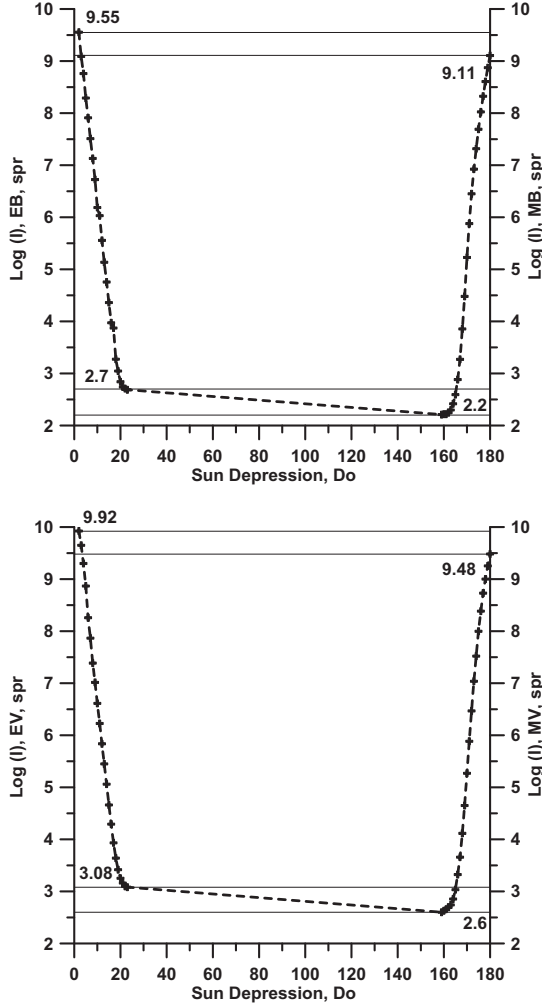
Fig. 3 The relation between the brightness $Log (I)$ in S_{10} unit in colors B and V (spring) and the sun's depression (D_o) from sunset to sunrise (0° to 180°).

Fig. 4 Morning and evening twilights drawn together in the same figure as a function of the depression from 0° to 180°. The progress of both phenomena is clear.

and at different altitudes, azimuths and meteorological conditions. A trial to fit the brightness depression relation by a 3rd degree polynomial was done.

2. Results

For Bahria in Egypt ($\varphi = 28° \, 42.94'$ N, $\lambda = 28° \, 59.99'$ E) at $a^o = 5$ and average azimuth within ($0° \leqslant A \leqslant 60°$), Fig. 1 and Fig. 2 show the evening and morning twilights brightness

(I) with depression D_o fitted by a relation of the form of Eq. (1),

$$Log(I) = c_0 + c_1 D_0 + c_2 D_0^2 + c_3 D_0^3 \tag{1}$$

where c_o–c_3 are the constants of the polynomial. The two sets of Fig. 1 are for summer (evening and morning), while those in Fig. 2 are the same for spring. The latter ranges between 0° and 60°. EB, EV and ER and MB, MV and MR are evening (E) and morning (M) in the blue (B), yellow (V) and red (R).

Interesting to us in these figures are two values; the intersection of the curve with the brightness axis expressed by c_o and the intersection of the tangent to the observed points (+) in the figures which represents the night sky brightness level. This region of the figures marked by (+) shows in almost all curves a trend of stability. It runs nearly parallel to the D_o axis. It shows very nearly no variation of the brightness with D_o.

Calculated values of c_o and the other constants are shown in Table 1. Values of c_o range between 7.86 and 9.493 in S_{10} units for summer and between 8.946 and 11.111 in S_{10} units for spring. We believe that this variation in the values of c_o is due to varying atmospheric conditions for each color band. In clear weather conditions, an average is most expressive.

We have reasons to consider an average $\overline{c_o}$ for all values of c_o in summer and spring, where $\overline{c_o}$ (summer) ≈ 9.06 and $\overline{c_o}$ (spring) ≈ 10 with average of nearly 9.5. The brightness axis is logarithmic and the units are in candels/ft^2. This value of the brightness (9.5) corresponds to 4.259×10^{-10} Joule. This is the brightness of the sky at sunset and sunrise.

Interesting also is the intersection of the tangent with the brightness axis. The average of intersection in summer is 2.667 in S_{10} unit, while it is 2.82 in S_{10} unit in spring. The difference is small, so that an average of 2.74 in S_{10} unit is representative. This value corresponds to 7.43×10^{-17} Joule, which represents the upper limit of the night sky brightness above which the number of photons begins to increase.

Figs. 3–5 show the brightness of both twilights (evening and morning) in the same diagram opposing each other (i.e. from 0° depression upward for evening and from 180° downward for the morning twilight). The figures are in the blue filter in summer and spring. A noticeable aspect of all the figures is the bending character shown at $D_o \approx 24°$ and at $D_o \approx 157°$ (23°). This bending is nearly sharp, indicating that an extrapolation can tie between both ends. This line, if continued to the brightness axis, cuts it at an average value at 2.68 in S_{10} unit giving brightness of the order of 7.5×10^{-17} Joule, which is equal to the night sky level above which the number of photons begins to increase but still not enough to reach the threshold of the eye. We believe that the brightness of the night all along lie around this value. Using the relation $m = -2.5\ Log\ b$, $m = -2.5\ Log\ (7.5 \times 10^{-10}$-Erg) ≈ 22.8 magnitudes. The generally accepted value is nearly 22.7 magnitude (Leinert et al. (1998)) which is not far from this value (22.8). Patat et al. (2006) studied the $UBVRI$ twilight brightness at dome C (Kenyon and Storey (2006)) and found that the night sky brightness levels are 22.25, 22.65, 21.5, 20.9 and 19.75 mag.arcsec^{-1} for $UBVRI$ respectively. They found that in all passbands, the night sky brightness level is reached at around zenith angle $\xi = 105°–106°$.

3. Color indices

Figs. 6 and 7 show the variations of the color indices CI [$(B–V)$, $(B–R)$ and $(V–R)$] for both evening and morning twilights for altitudes 5°, 30° and 60° and for an azimuth averaged over a range from 0° to 60° given as a function of the depression of the sun below the horizon, D_o. Each figure contains two sets for evening and morning twilights for the sake of comparison. The lines are least squares solutions of a 4th degree polynomial as:

$$CI = c_o + c_1 D_o + c_2 D_o^2 + c_3 D_o^3 + c_4 D_o^4 \qquad (2)$$

where the c_o–c_4 are the constants of the polynomial. All solutions in Figs. 6 and 7 show the same trend. A minimum is shown in all curves at a depression $11° \leqslant D_o \leqslant 12°$. The sky is highly reddened for morning twilight at this depression (nautical twilight). Then, reddening slightly decreases on both sides of the minimum for the sake of the blue color, though red background is present (indicated by positive values $(V–R)$ and $(B–R)$). Of interest to us is the stability region shown clearly by the points, where the curves start to gather and run parallel to the depression axis.

Some of the spring color index curves show a general trend nearly opposite to that of summer. They show a minimum reddening nearly in the same range of depression $10° \leqslant D_o \leqslant 12°$. The stability region is shown in most figures. We believe that this stability region is the same as the region shown in Figs. 1 and 2, which corresponds to the upper limit of the night sky. Table 2 gives approximate values of the depression of the sun below the horizon for the stability region in degrees. The depression at the beginning of the
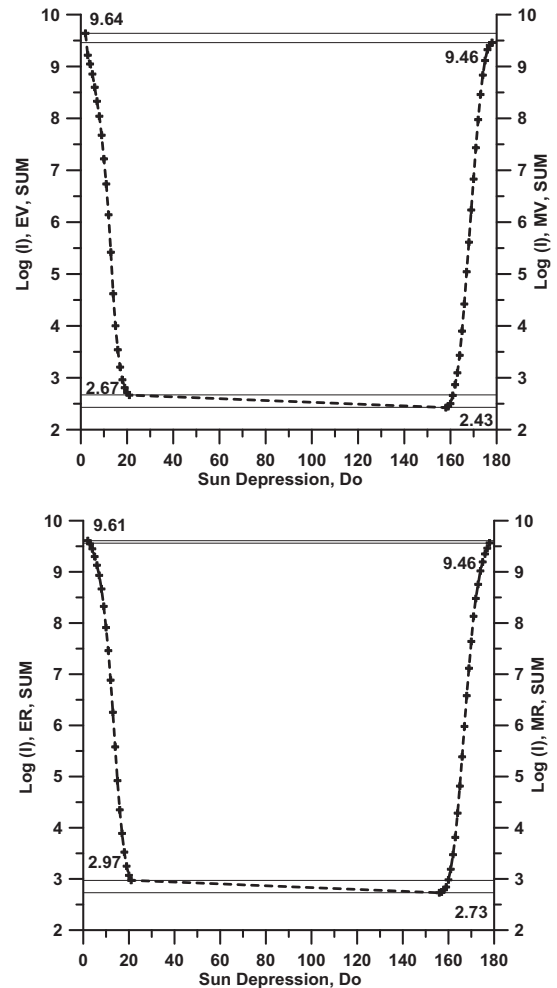

Fig. 5 The relation between the brightness $Log\ (I)$ in S_{10} unit in colors B and V (summer) and the sun's depression (D_o) from sunset to sunrise (0° to 180°).
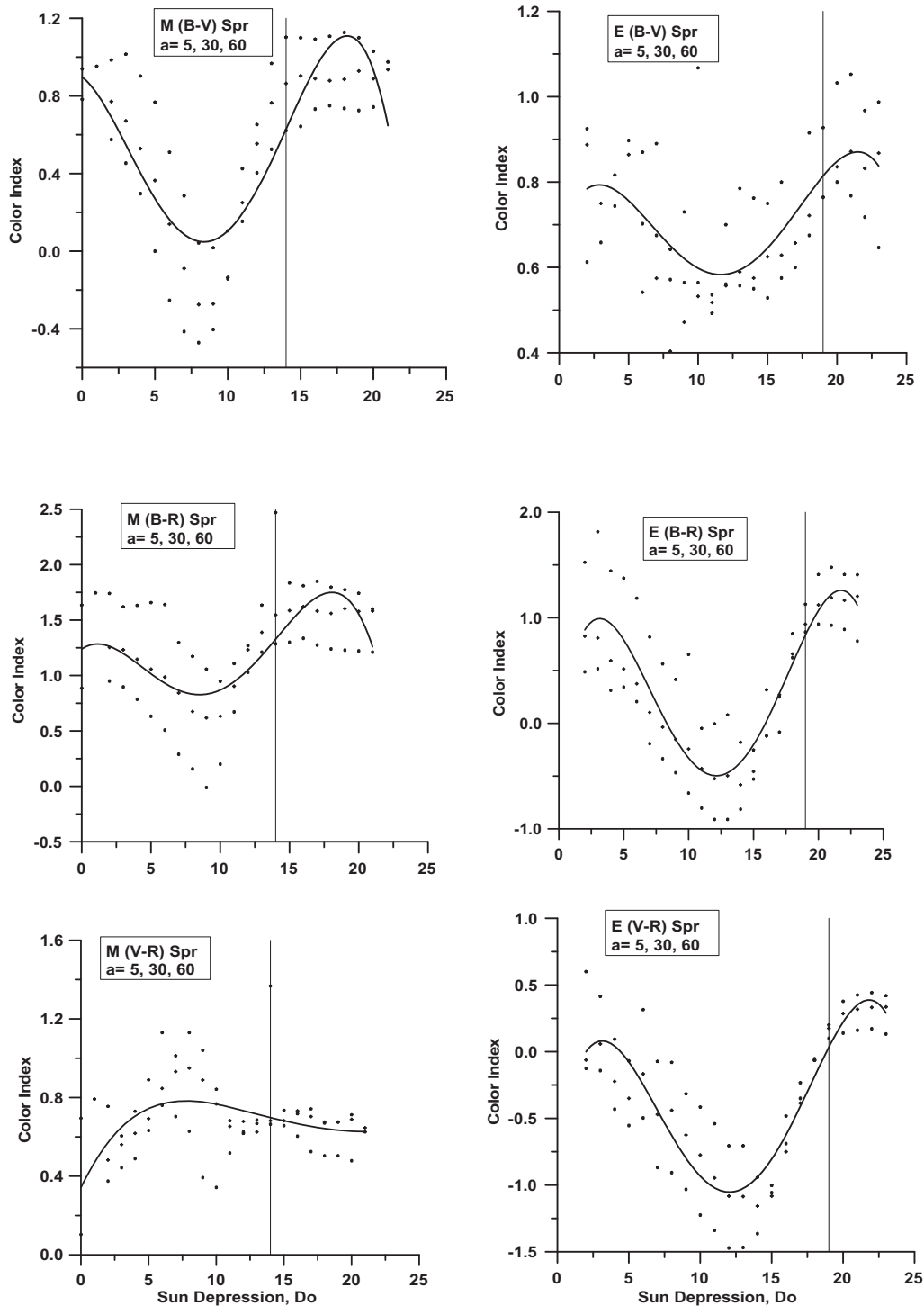
Fig. 6 The relation between different color indices (*B–V*), (*B–R*) and (*V–R*) and the sun depression (*D_o*) at Bahria, for evening (*E*) and morning (*M*) twilights azimuth averaged over (0° ⩽ *A* ⩽ 60°). The solid line is a 4th polynomial fit averaged over (*a* = 5°, 30° and 60°).

stability region confirms the dusk phenomenon after the very early twilight.

Also, according to Figs. 6 and 7, the beginning of twilight in spring occurs at depression values $D_o = 14°$, while it occurs at depression values $D_o = 15°$ in summer especially at (*B–V*) bands. The evening twilight occurs in both seasons at depression values lying in $18° \leqslant D_o \leqslant 19°$.

Table 3 gives the coefficients of the 4th degree polynomials to fit the color indices as a function of the sun's depression (*D_o*). The fourth degree polynomial can fit the color index curves for evening (*E*) and morning (*M*) in different color bands (*B–V*), (*B–R*) and (*V–R*) in spring (Spr.) and summer (Sum.). In spring, the values of c_o for *M(B–V)* is 0.9, for *M(B–R)* is 1.24, for *E(B–V)* is 0.67 and for *E(B–R)* is 0.0054.
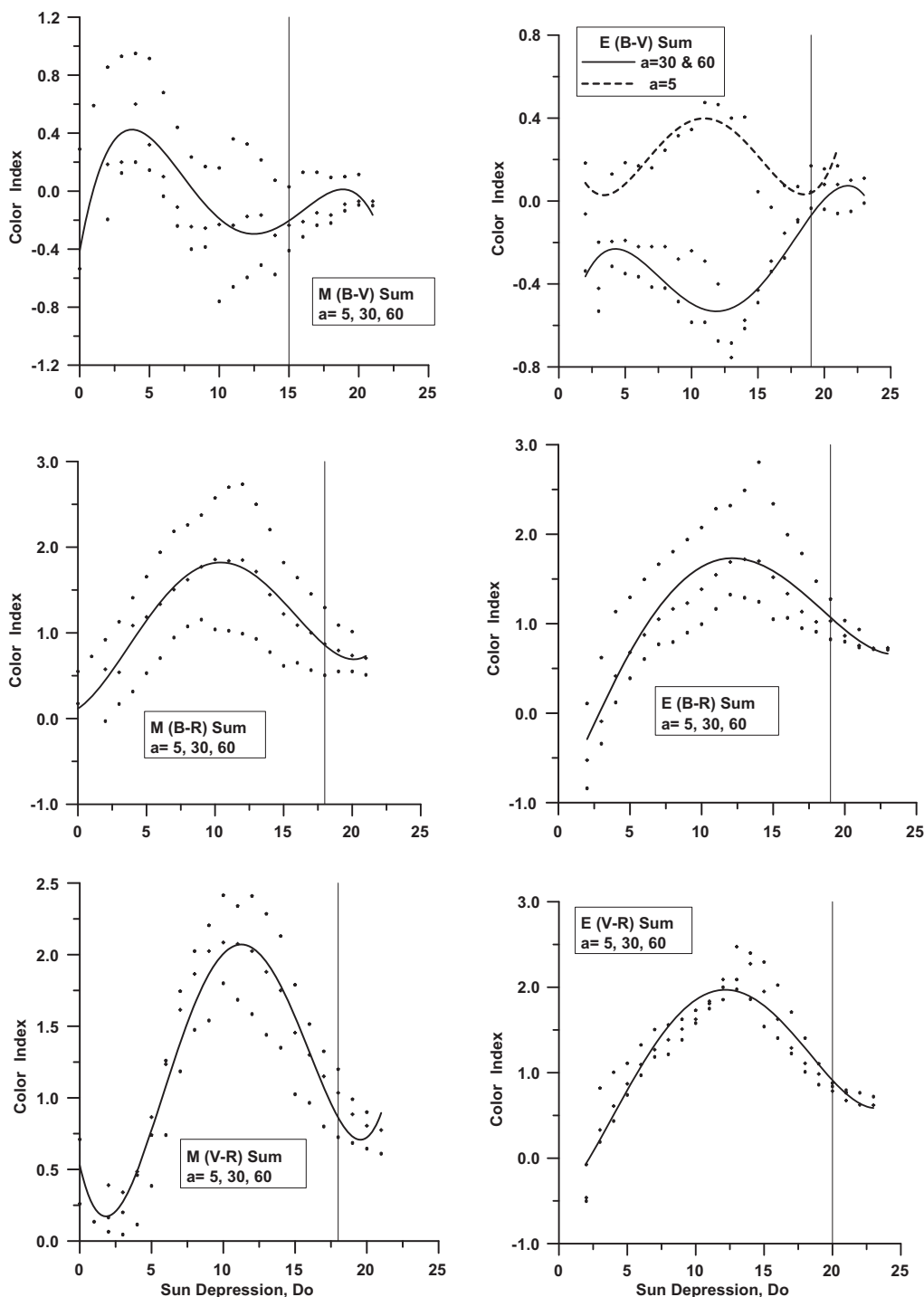
Fig. 7 The relation between different color indices (B–V), (B–R) and (V–R) and the sun depression (D_o) at Bahria, for evening (E) and morning (M) twilights azimuth averaged over ($0° \leqslant A \leqslant 60°$). The solid line is a 4th degree polynomial fit averaged over a range of altitude ($a = 5°$, $30°$ and $60°$).

The color of the sun (B–V) is 0.65 and the value of (V–R) is 0.74 Patat et al. (2006).

Generally from Figs. 6 and 7 and Table 3, the average values of (B–V) and (B–R) color indices indicate that the twilight sky is redder than the sun at the direction of the sunset when $D_o > 14°$ and bluer than the sun for all other

given values of $a°$, $A°$ and D_o. The (B–V) color index value equals zero at $A° = 0$ for $a = 0°$ and $20°$ (i.e. minimum purple hue where $B = V$). However, this minimum value gives way to reddening with an increase in the sun depression which is also noticed at almost all other directions in the sky.

Table 2 Values of depression of the sun below the horizon for the end and beginning of twilight in different color bands (B–V), (B–R) and (V–R) at spring and summer seasons.

Color band	Evening spring	Morning spring	Evening summer	Morning summer
(B–V)	19°	14°	19°	15°
(B–R)	19°	14°	19°	18°
(V–R)	19°	14°	20°	18°

Table 3 The constants of the polynomial for evening (E) and morning (M) in different color bands (B–V), (B–R) and (V–R) for summer and spring seasons. No. is the number of observations and C.C. is the correlation coefficient.

Color band	No.	c_o	$c_1 \ deg^{-1}$	$c_2 \ deg^{-2}$	$c_3 \ deg^{-3}$	$c_4 \ deg^{-4}$	C.C.
E(B–V) Spr.	62	0.6722	0.0957	−0.023	0.0016	−3.3 E−005	0.62
M(B–V) Spr.	65	0.8968	−0.055	−0.032	0.0041	−0.00012	0.82
E(B–R) Spr.	66	0.00545	0.7201	−0.161	0.0107	−0.0002	0.86
M(B–R) Spr.	66	1.237	0.0904	−0.048	0.0048	−0.00013	0.63
E(V–R) Spr.	66	−0.6749	0.5536	−0.124	0.0083	−0.000168	0.87
M(V–R) Spr.	65	0.3421	0.1431	−0.0155	0.0006	−8.8 E−006	0.51
E(B–V) Sum.	20	0.4728	−0.3106	0.0684	−0.005	0.000113	0.78
E(B–V) Sum.	44	−0.8128	0.33014	−0.060	0.0038	−7.5 E−005	0.85
M(B–V) Sum.	65	−0.4128	0.5296	−0.1059	0.007	−0.000149	0.60
E(B–R) Sum.	64	−1.0043	0.3562	0.0036	−0.002	4.5 E−005	0.81
M(B–R) Sum.	65	0.11616	0.0394	0.1048	−0.004	0.000112	0.73
E(V–R) Sum.	64	−0.4978	0.1632	0.035	−0.0036	8 E−005	0.93
M(V–R) Sum.	65	0.52897	−0.425	0.1453	−0.0114	0.000262	0.93

4. Comparison and conclusion

For evening twilight, we find a minimum value in the color index (CI) curves at $D_o = 12.5°$. The color index (CI) is found to be in the range between 2.5 and 3 of brightness units. A decrease on both sides of the CI toward large and small depressions is seen indicating a red background. This red color decreases on both sides of the maximum although being positive. No change of the maximum values is noticed with the azimuth.

The (B–R) curves show positive maximum values in summer at $11° \leqslant D_o \leqslant 13°$ with a decrease on both sides and vice versa in spring. The stability is reached at $D_o = 20°$ as in both (B–R) and (V–R) set. Values of the CI at $D_o = 20°$ are still positive which indicates a red background sky. In Abu-Simbel (22° 20′ N, 31° 38′ E), Asaad et al. (1977) found the maximum at depressions of 12° and 14°. Our results can be in a good agreement with Rosenberg (1966).

For morning twilight, the (B–V) color index curves show minimum (CI) values with positive (B–V) at D_o around 8°. This can denote a dominating yellow color of the sky till $D_o \approx 8–10°$, where the sky is as bright in the yellow as in the blue. Stability is reached at $D_o = 12–14°$. Interesting are the values where B is nearly equal to V. The sky is affected nearly equal with both B and V colors. However, a trend toward yellow color appears at less depression. The (V–R) curves show minimum values with positive (V–R) in the range $10° \leqslant D_o \leqslant 12.5°$ in spring, while they show maximum values with positive (V–R) in the same range. At this depression, red color disperses all over the sky as a background. As the depression increases, the (V–R) decreases in spring morning to give color stability beginning from $D_o = 15°$ with (V–R) values around 1. Values around $V \approx R$ give rise to reddened background which

appears to continue all night long. This is comparable to the results of Assad and Mikhail (1967).

A third degree polynomial fitting for the relation between the brightness of both twilights and the depression of the sun below the horizon was found to be very reliable. The c_o constant has resulted in 2.259×10^{-10} Joule at sunset and 7.43×10^{-17} Joule at the end of twilight. This denotes ratio of nearly 10^6 in brightness between both values. The tangent to the saturation points of our observations intersects the brightness axis at c value of 2.742 of S_{10} units corresponding to 7.43×10^{-17} Joule nearly equal to the night sky brightness. A plot of both evening and morning twilights in the same diagrams indicates a sharp bending at $D_o = 24–157°$. Both bends occur nearly at 2.68 in S_{10} units again giving a value very nearly equal to the night sky brightness level. An extrapolation between both ends corresponding to a brightness value nearly equals to the threshold of normal eye. This gives a magnitude of 25. The brightness of the night sky is nearly ∼22.7 magnitude.

A fourth degree polynomial was found to fit color index curve. Our color index curves are not far from those reported by Rosenberg (1966), Asaad et al. (1977), Nawar (1983), Issa et al. (2011), Hassan et al. (2013). The saturation shown in the brightness curves is also shown in the color index curves. Lines drawn parallel to the color index axes for morning twilight are drawn just at the beginning of the stability region, while for evening twilight are drawn at the end of the stability region.

For morning twilight, the stable region was found to begin between 14° and 15.5° depression, while it was found to begin between 18° and 19° for evening twilight. Therefore, the dawn declares itself at $D_o \leqslant 15°$, while the nightfall declares itself at $D_o \leqslant 18°$.

References

Aden, B., Meinel, M., 1991. Sunsets, Twilight and Evening Skies. Cambridge University Press, p. 63.

Assad, A.S., Mikhail, J.S., 1967. Brightness of the twilight and its variation at Misallat. Helwan Observatory Bull. 68.

Asaad et al, 1974. Atmospheric transparency at Misallat, Helwan and Daraw. Helwan Observatory Bull. 109.

Assad, A.S., Mikhail, J.S., Abdel Shaheed, S.N., 1977. Sky color variation during the twilight period at Helwan and Daraw. Helwan Observatory Bull. 144.

Belikov, Yu.E., 1996. Modeling of the twilight sky brightness using a numerical solution of the radiation transfer equation. J. Atmos. Terr. Phys. 58 (16), 1848–1849.

McGillivray, Donald, 1987. Physics and Astronomy. Macmillan Education LTD, London.

Gadsden, M., 1966. Twilight observation institute for telecommunication science and astronomy, environmental, scientific service administration, boulder, colorado. Geophys. Res..

Hardie, B.H., 1962. Astronomical Techniques. In: Hiltner, W.A. (Ed.). University of Chicago Press.

Hassan, A.H., Hassanin, N.Y., Abdel-Hadi, Y.A., Issa, I.A., 2013. Time verification of twilight begin and end at Matrouh of Egypt. NRIAG J. Astron. Geophys. 2, 45–53.

Issa, I.A., Hassan, A.H., 2008a. Transparency of the night sky at Bahria/Egypt I. NRIAG J. Astron. Astrophys. Special issue, 383–397.

Issa, I.A., Hassan, A.H., 2008b. Evening and morning twilights at Bahria/Egypt II. NRIAG J. Astron. Astrophys. Special issue, 399–411.

Issa, I.A., Hassan, A.H., 2008c. Eye criteria and times of end and begin of twilights Bahria/Egypt III. NRIAG J. Astron. Astrophys. (Special issue), 413–423.

Issa, I.A., Hassanin, N.Y., Hassan, A.H., Yasser, A., Abdel-Hadi, 2011. Atmospheric transparency, twilight brightness and color indices at Kottamia of Egypt. NRIAG J. Astron. Astrophys. Special issue, 379–398.

Kenyon, S.L., Storey, J.W.V., 2006. A Review of Optical Sky Brightness and Extinction at Dome C. Antarctica, Publications of the Astronomical Society of the Pacific 118, 489–502.

Leinert, Ch. et al, 1998. The 1997 reference of diffuse night sky brightness. Astron. Astrophys. Suppl. Ser. 127, 1–99.

Mikhail, J.S., 1979. Clear air monochromatic extinction coefficient for the site of Kottamia observatory, Egypt. Helwan Observatory Bull. Egypt 186 (I).

Mikhail, J.S., 1979. Seasonal atmospheric extinction. Astrophys. Space Sci. 66, 349–352 (II).

Nawar, S., 1983. Sky twilight brightness and color during high solar activity, Earth, Moon and Planets, 29, pp. 99–105.

Nawar, S., 1995. Variation of evening zenith sky twilight brightness and color at Abu-Simbel during spring, Earth, Moon and Planets, 70, pp. 123–131.

Patat, F., Ugolnikov, O.S., Postylyakov, 2006. UBVRI twilight sky brightness at ESO-Paranal. Astron. Astrophys. 455, 385–393.

Richard, H., Blackwell, 1946. Contrast thresholds of the human eye. J. Opt. Soc. Am 36 (11), 624–643.

Roach, F.E., Gordon, J.L., 1973. The Light of the Night Sky. D. Reidel Publications Comp., U.S.A..

Rosenberg, G.V., 1966. Twilight. plenum press, New York.

Valberg, A., 2005. Light Vision Color. John Wiley & Sons Ltd.